Passive translocation of phospholipids in asymmetric model membranes: Solid-state ^{1}H NMR characterization of flip-flop kinetics using deuterated sphingomyelin and phosphatidylcholine

Authors

Hirofumi Watanabe,[1] Shinya Hanashima,[1,2,*] Yo Yano,[1] Tomokazu Yasuda,[1,3] Michio Murata[1,3,*]

Affiliations

[1]Graduate School of Science, Osaka University, 1-1 Machikaneyama, Toyonaka, Osaka 560-0043, Japan.

[2] Graduate School of Engineering, Tottori University, 4-101 Koyama-cho Minami, Tottori 680-8550, Japan

[3]Forefront Research Center, Graduate School of Science, Osaka University, Toyonaka, Osaka 560-0043, Japan

Corresponding Authors hanashima@tottori-u.ac.jp (S. H.) and murata@chem.sci.osaka-u.ac.jp (M.M.)

Abstract

Although lateral and interleaflet lipid-lipid interactions in cell membranes play roles in maintaining asymmetric lipid bilayers, the molecular basis of these interactions is largely unknown. Here we established a method to determine the distribution ratio of phospholipids between the outer and inner leaflets of asymmetric large unilamellar vesicles (aLUVs). The trimethylammonium group, $(CH_3)_3N^+$, in the choline headgroup of *N*-palmitoyl-sphingomyelin (PSM) and 1,2-dioleoyl-*sn*-glycero-3-phosphatidylcholine (DOPC) gave rise to a relatively sharp signal in magic angle spinning solid-state ^{1}H NMR (MAS-ss-^{1}H NMR). PSM and DOPC have the same headgroup structure, but one phospholipid was selectively observed by deuterating the trimethylammonium group of the other phospholipid. The addition of Pr^{3+} to the medium surrounding aLUVs selectively shifted the chemical shift of the $(CH_3)_3N^+$ group in the outer leaflet from that in the inner leaflet, which allows the estimation of the interleaflet distribution ratio of unlabeled lipid in aLUVs. Using this method, we evaluated the translocation of PSM and DOPC between the outer and inner leaflets of the cholesterol-containing aLUVs, with PSM and DOPC mostly distributed in the outer and inner leaflets, respectively, immediately upon aLUV preparation, and flip and flop rates of approximately 2.7 and 6.4 $\times 10^{-6}$ s^{-1}, respectively. During the passive symmetrization of the aLUVs, the lipid translocation rate was decreased due to changes in the membrane order, probably through the formation of the registered liquid-ordered domains. Comparison of the result with that of symmetric LUVs revealed that lipid asymmetry may not significantly affect the lipid translocation rates while lateral lipid-lipid interaction may be a dominant factor in lipid translocation under these conditions. These findings highlight the importance of considering the effects of lateral lipid interactions within the same leaflet on lipid flip-flop rates when evaluating the asymmetry of phospholipids in the cell membrane.

Introduction

The asymmetry of the cell membrane bilayer structure, in which the outer and inner leaflets exhibit different lipid compositions, is maintained by homeostasis.[1] In the mammalian plasma membrane, phosphatidylcholine (PC), sphingomyelin (SM), and glycosphingolipids that predominantly possess saturated acyl chains are largely distributed in the exoplasmic-leaflet.[2,3] By contrast, phosphatidylserine (PS), phosphatidylethanolamine (PE), and phosphatidylinositol (PI) with unsaturated acyl chains are mostly present in the cytosolic leaflet.[2,4,5] The coupling of the outer and inner leaflets is thought to play certain roles in cellular homeostasis and intercellular communication. Membrane asymmetry, which is homeostatic in yeast cells, maintains normal membrane concentrations of ergosterol.[6] In the presence of cholesterol (Cho), sphingolipids including SM in the outer-leaflet of cell membranes form lipid rafts as a functional domain, whereas PI and phosphatidylinositol phosphates (PIPs) are presumably localized on the inner-leaflet side of lipid rafts.[7,8,9] Membrane asymmetry is essential for cell viability, as shown in the retention of sterols in

yeast cell membranes.[6] Disturbance of this asymmetry such as the exposure of PS to the exoplasmic-leaflet is known to be a signal of cell apoptosis[10] and seen in exosomes produced by cancer cells.[11] PEs exposed in the outer leaflets are involved in membrane fusion by inducing negative curvatures.[12]

Asymmetric distribution of phospholipids occurs during biosynthesis and transport from the intracellular system to the plasma membrane. Lateral and trans-bilayer lipid interactions are key factors controlling the thermodynamic equilibrium that reduces bilayer asymmetry.[13,14] The membrane-associated enzymes, so-called flippases and flopases, translocate phospholipids to the opposite leaflet to overcome the thermodynamic scrambling of bilayer asymmetry, whereas scramblases promote scrambling.[15,16] Both thermodynamic equilibrium and ATP-driven mechanisms are at work in the homeostatic asymmetric distribution of membrane lipids under physiological conditions.

One of the drawbacks of artificial vesicles commonly used in biophysical studies is the symmetric lipid distribution of each leaflet. Thus, several methods have been developed for preparing asymmetric bilayers:[17] overlaying the two different lipid monolayers together,[18] the water-oil interface,[19,18] Ca^{2+}-induced flipping of phosphatidylserine,[20,21] and the outer-leaflet selective enzymatic transformation.[22,23] Among them, the method based on methyl-cyclodextrin-mediated lipid exchange has widely been used to prepare asymmetric unilamellar vesicles (aLUVs).[24] The lipid composition of each leaflet of aLUV is estimated indirectly using fluorescent probes[25] and chemical modifications.[26]

In model-membrane studies of leaflet-specific distribution and translocation of phospholipids, lipid-type fluorescence probes are often used to observe the flip-flop[25] although bulky hydrophobic fluorophores sometimes alter the intrinsic behavior of lipids. Using non-labeled phospholipids, therefore, Liu and Conboy[27,28] measured their flip-flop kinetics by vibrational spectroscopy for planar supported bilayers. They reported rate constants of phospholipids (k), which is the number of flips or flops of phospholipids that occur per second, are in the order of 10^{-3} to 10^{-4} s^{-1} in the symmetric bilayers of saturated PCs in the liquid phase, and in the order of 10^{-5} s^{-1} in the DSPC/Cho (85: 15) bilayers; these rate constants correspond to the half-lives of a few minutes to several hours.[27, 28] By contrast, molecular dynamics (MD) simulations reported that the flip-flop rate constant of DPPC at 50 °C is estimated to be much slower and ranges from 10^{-6} to 10^{-7} s^{-1}, with half-lives corresponding to tens of hours to several days.[29]

To distinguish the occurrence of lipid in the outer leaflet from those in the inner leaflet (and inside) of vesicles, the paramagnetic lanthanide-induced chemical shift (LIS) of NMR signals has been used to selectively observe the ^1H signal originating from the trimethylammonium group of the headgroup choline.[30,31] The paramagnetic relaxation enhancement of phospholipids, which has been used for estimating the depth of bound molecules in lipid bilayers,[32] is also adopted to evaluate the asymmetric binding of peptides.[33] Because lanthanide ions do not permeate the lipid bilayers, the ions added to the vesicle suspension are thought to selectively interact with the phospholipids distributed in the outer-

most leaflet.[33] When the ^{1}H NMR spectrum of vesicles is measured on a solution NMR instrument, the signal width is significantly broadened due to ^{1}H-^{1}H magnetic dipole-dipole coupling within an LUV-bound phospholipid molecule with low mobility. Additionally, the presence of paramagnetic lanthanide ions could further interfere with quantitative measurements of peak area.[34,35]

In this study we examined the flip-flop kinetics of phospholipids bearing choline headgroups in aLUV membranes using solid-state ^{1}H NMR spectroscopy. Magic angle spinning (MAS) was employed to enhance spectral resolution by reducing the chemical shift anisotropy and magnetic dipolar interactions. Although the MAS technique has often been used to separate multiple ^{13}C NMR signals of membrane-bound peptides[36] and antibiotics,[37] its application for detecting ^{1}H signals is limited mainly due to the high dipolar interaction of ^{1}H nuclei. In this aspect, the choline group is suitable for ^{1}H NMR experiments because of its high mobility and low dipolar interaction with the surrounding ^{1}H nuclei. aLUVs composed of PSM in the outer leaflet (PSM^{out}) and DOPC in the inner leaflet (DOPC^{in}) were prepared as a model for biological membranes, where γ-d_9-PSM or γ-d_9-DOPC (Fig 1) was introduced instead of unlabeled lipids to eliminate these signals and to highlight the $(CH_3)_3N^+$ signal of the unlabeled lipids. Addition of $Pr(NO_3)_3$ to the surrounding medium induced LIS that distinguished the $(CH_3)_3N^+$ signals on the outer leaflet from those on the inner leaflet. The NMR results demonstrated that the asymmetric distributions of PSM and DOPC were gradually disrupted at 40 °C with the initial rate constants of 2 to 7 $\times 10^{-6}$ s^{-1} (40 °C), reaching equilibrium in about 100 h. Differences in the flip-flop rate constant of PSM and DOPC were examined under symmetric and asymmetric membrane conditions. Whereas strong correlation of the flip-flop rate with lateral lipid–lipid interactions was observed in both conditions, the composition of the interleaf lipids had only a slight effect on the flip-flop kinetics.

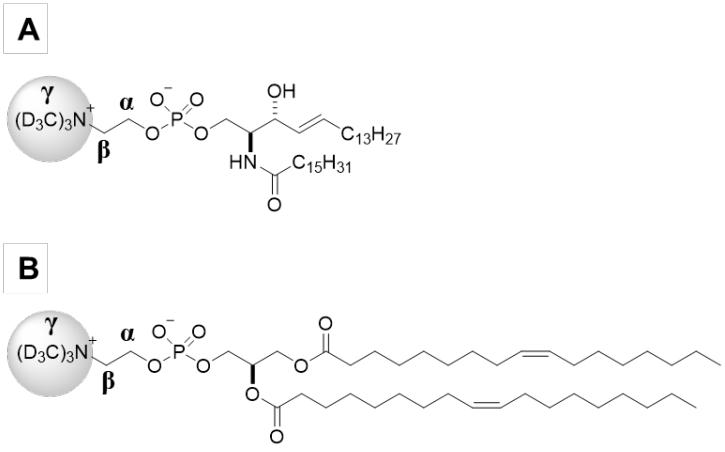

Figure 1. Chemical structures of γ-d_9-PSM (A) and γ-d_9-DOPC (B).

EXPERIMENTAL SECTION

General Materials. Palmitoyl-2-oleoyl-sn-glycero-3-phosphocholine (POPC) and 1,2-dioleoyl-

sn-glycero-3-phosphocholine (DOPC) were purchased from Yuka Sangyo (Tokyo, Japan). The egg SM was purchased from Nagara Science (Gifu, Japan). 1,2-dioleoyl-sn-glycero-3-phosphoethanolamine (DOPE), cholesterol (Cho), and $Pr(NO_3)_3$ $6H_2O$ were purchased from Nacalai Tesque (Kyoto, Japan). Methyl-α-cyclodextrin (MαCD) was purchased from AraChem (Netherlands). Palmitoyl sphingomyelin (PSM) was isolated at 99% purity from egg SM by preparative reverse-phase high-performance liquid chromatography (HPLC) (Discovery C18 column, Supelco, Bellefonte, PA) using methanol as the eluent. γ-d_9-PSM and γ-d_9-DOPC were synthesized in our laboratory and synthetic procedures are described in the Supporting Information section.

Preparation of symmetric LUVs. Symmetric LUVs (sLUVs) were prepared according to a previously reported protocol.[38,39] Briefly, appropriate amounts of lipids in $CHCl_3$ and MeOH were dispensed into glass tubes. The organic solvent was evaporated under a stream of Ar, and the remaining lipid films were exposed to a high vacuum overnight. Dried lipid films were hydrated with D_2O (or 0.9% NaCl in D_2O) for POPC/Cho (7:3) LUVs or D_2O for acceptor LUVs at 65 °C for 30 min and vortexed vigorously. The solution was then subjected to five freeze-thaw cycles to obtain multilamellar vesicles (MLVs). Finally, the resultant MLVs were filtered 11 times through a polycarbonate filter with a pore size of 100 nm (Whatman) at 65 °C using a Mini-Extruder set (Avanti Polar Lipids, Alabaster, AL). The resultant LUV suspensions were concentrated using Amicon Ultra-2 (100 kDa) (Merck Millipore) at 4000 ×g for 120 min at 4 °C. Appropriate amounts of $Pr(NO_3)_3$ •$6H_2O$ dissolved in D_2O (or in D_2O containing 0.9% NaCl) were added to the LUVs suspensions to obtain a final concentration of 1 mM Pr^{3+}.[19] The concentrated sLUVs suspensions, with or without Pr^{3+}, were then carefully transferred to Bruker BL4 HR-MAS Kel-F inserts. In the NMR spectra in Fig. 1, we used 0.9% NaCl in D_2O to prepare sLUVs following usual physiological conditions. For measuring flip-flop rates with aLUVs (and sLUVs), we used D_2O to obtain reproducible peak areas in NMR experiments.

Preparation of aLUVs. aLUVs were prepared according to previously reported protocols with some modifications.[24] aLUVs composed of PSM^{out} and $DOPC^{in}$ with Cho in both leaflets were prepared from donor MLVs composed of PSM and acceptor LUVs composed of DOPC and Cho. For preparation of donor MLVs, 12 μmol of unlabeled PSM or γ-d_9-PSM in MeOH was dispensed into glass tubes. The organic solvent was evaporated under a stream of Ar, and the remaining lipid films were exposed to high vacuum for at least 1 h. The dried film was then hydrated with 400 μL of a 25% sucrose solution by vigorous vortexing and incubated at 65 °C in a water bath for 20 min. To this donor MLV suspension, 100 μL of 0.6 M MαCD in 25% (w/w) sucrose solution was added, and the mixture was incubated at 65 °C for 2 h. For acceptor LUVs, 6 μmol of a lipid mixture composed of 2:1 DOPC/Cho (mol/mol) or 2:1 γ-d_9-DOPC/Cho (mol/mol) in $CHCl_3$ was dispensed into glass tubes. The samples were dried as described above and then hydrated with D_2O (500 μL) at 65 °C in a water bath

for 20 min; D_2O was used for MAS-ss-^{1}H NMR measurements. The suspension was then subjected to five freeze-thaw cycles to obtain MLVs. Finally, to prepare LUVs, the resulting MLVs were filtered 11 times through a polycarbonate filter with a pore size of 100 nm (Whatman) at 65 °C using a Mini-Extruder set (Avanti Polar Lipids, Alabaster, AL). The resultant acceptor LUVs were concentrated with Amicon Ultra-2 (100 kDa) (Merck Millipore) at 4000 ×g for 40 min at 20 °C and diluted with D_2O (12 mM lipid conc.). The acceptor LUV suspension with the lipid concentration of 12 mM (500 μL) was mixed with 24 mM donor MLV suspension (500 μL) that contained MαCD and incubated at 30 °C for 50 min. The mixtures were then carefully added to an 8% (w/w) sucrose solution (2 mL) and subjected to ultracentrifugation at 233,000 ×g for 30 min at 20 °C using Optima MAX ultracentrifuge (Beckman Coulter) and MLA-55 rotor (Beckman Coulter). After removing the donor mixtures in the underlayer (approximately 1 mL), the suspension was subjected to ultracentrifugation at 233,000 ×g for 30 min at 20 °C, and the supernatant containing aLUVs was separated from the donor MLV pellets. The lipid compositions of aLUVs were separately confirmed by solution ^{1}H NMR spectroscopy, as described in Supporting Information.

The LUVs used as 'symmetric' vesicles were prepared with the configuration of PSM^{out}/γ-d_9-PSM^{in} or γ-d_9-DOPC^{out}/DOPC^{in} (see Graphic Abstract) by a similar protocol to that used for asymmetric vesicles. The Cho contents in both of the symmetric vesicles ranged from 18 to 28 mol% were estimated by solution ^{1}H NMR as described in Supporting Information.

For MAS-ss-^{1}H NMR samples, aLUVs present in the supernatant after the ultracentrifugation were concentrated, and then washed with D_2O (2 mL) by using Amicon Ultra-2 (100 kDa) at 4000 ×g for 40 min at 4 °C. For a flip-flop experiment, the obtained aLUVs were aliquoted and incubated for 0–180 h at 40 °C. Then, a solution of $Pr(NO_3)_3 \cdot 6H_2O$ in D_2O was added (1 mM Pr^{3+} in final concentration). To reduce sample volume suitable for NMR measurements, the aLUVs suspension was concentrated with Amicon Ultra-0.5 (100 kDa) (Merck Millipore) at 14,000 ×g for 40 min at 4 °C, and retained LUV suspension was transferred carefully to Bruker BL4 HR-MAS Kel-F inserts (4 mm). The total concentration of lipids in the NMR experiments was estimated by ultra-performance liquid chromatography coupled to electrospray ionization (UPLC-ESI-MS) analysis (see Supporting Information). For TMA-DPH (and DPH) anisotropy measurements,-MilliQ water was used instead of D_2O. Details of the anisotropy measurements is described in Supporting Information.

Preparation of ss-NMR and anisotropy samples. For MAS-ss-^{1}H NMR samples, aLUVs present in the supernatant after the ultracentrifugation were concentrated, and then washed with D_2O (2 mL) using Amicon Ultra-2 (100 kDa) at 4000 ×g for 40 min at 4 °C. For a flip-flop experiment, the obtained aLUVs were aliquoted and incubated for 0–180 h at 40 °C. A solution of $Pr(NO_3)_3 \cdot 6H_2O$ in D_2O was then added (1 mM Pr^{3+} as final concentration in NMR measurement). To reduce sample volume suitable for NMR measurements, the aLUVs suspension was concentrated with Amicon Ultra-

0.5 (100 kDa) (Merck Millipore) at 14,000 ×g for 40 min at 4 °C, and retained LUV suspension was transferred carefully to Bruker BL4 HR-MAS Kel-F inserts (4 mm). The translocation of lipid during preparation of NMR samples and NMR measurement was considered negligible, since the temperatures of these steps were significantly lower than the incubation temperature. Therefore, the effect of lanthanide ions on the lipid translocation reported by Cheng and Conboy was not taken into account in these experiments since lanthanide ions exhibit slower lipid exchange.[40] The total concentration of lipids in the NMR experiments was estimated by ultra-performance liquid chromatography coupled to electrospray ionization (UPLC-ESI-MS) analysis (see Supporting Information).

For trimethylammonium-diphenylhexatriene (TMA-DPH) and diphenylhexatriene (DPH) anisotropy measurements, MilliQ water was used instead of D_2O. Details of the anisotropy measurements is described in Supporting Information.

MAS-solid-state ^{1}H NMR. Solid-state ^{1}H-NMR spectra under MAS conditions were acquired on a Bruker AVANCE400 spectrometer at 400 MHz and a Bruker AVANCE600 spectrometer at 600 MHz for the ^{1}H frequency. A Bruker standard pulse program zg30 was used with a 90° pulse width of 4 μs and recycle delay of 5 s. The MAS rate was set to 12 kHz, unless otherwise specified. Spectra were collected at 30 °C, and the number of scans ranged from 500 to 3,000.

Distribution and flip-flop rate of PSM and DOPC. The flip-flop rates of phospholipids were estimated according to previous reports,[27] with slight modifications. The fractions of PSM in the outer-leaflet ($f_{PSM}^{Outer}(t)$) and DOPC in the inner-leaflet ($f_{DOPC}^{Inner}(t)$) of aLUVs upon incubation for time t were determined for the samples composed of PSM^{out}/γ-d_9-DOPC^{in} and γ-d_9-PSM^{out}/DOPC^{in} bilayers, respectively, based on equations (1) and (2).

$$f_{PSM}^{Outer}(t) = \frac{R_{shifted}}{R_{shifted}+R_{unshifted}} \quad (1)$$

$$f_{DOPC}^{Inner}(t) = \frac{R_{unshifted}}{R_{shifted}+R_{unshifted}} \quad (2)$$

where $R_{shifted}$ and $R_{unshifted}$ are the relative areas of the shifted and unshifted $(CH_3)_3N^+$ peaks in the MAS 1H-NMR spectra, respectively, in the presence of Pr^{3+}. The peak areas were estimated by fitting Lorentz functions upon spectral deconvolution using an in-house Excel program (Microsoft Corporation, WA, USA).
as estimated by fitting with Lorentz functions upon spectral deconvolution by in house program using Excel (Microsoft Corporation, WA, USA).

The lipid flip-flop rates (k_{PSM} and k_{DOPC}) were determined directly from the time dependent decay of fractions $f_{PSM}^{Outer}(t)$ and $f_{DOPC}^{Inner}(t)$, the time-dependent decay of $f_{PSM}^{Outer}(t)$ and $f_{DOPC}^{Inner}(t)$ (entire

data are shown in Supporting Information).[3] $f_{PSM}^{Outer}(t)$ and $f_{DOPC}^{Inner}(t)$ were fitted with the following equations (Eq. 3 and 4) using OriginPro9.1 (OriginLab Corporation, MA, USA).

$$\Delta f_{PSM}^{Outer}(t) = \frac{f_{PSM}^{Outer}(t) - f_{PSM}^{Outer}(t_{max})}{f_{PSM}^{Outer}(0) - f_{PSM}^{Outer}(t_{max})} = \exp(-2k_{PSM}t) \quad (3)$$

$$\Delta f_{DOPC}^{Inner}(t) = \frac{f_{DOPC}^{Inner}(t) - f_{DOPC}^{Inner}(t_{max})}{f_{DOPC}^{Inner}(0) - f_{DOPC}^{Inner}(t_{max})} = \exp(-2k_{DOPC}t) \quad (4)$$

$f_{PSM}^{Outer}(0)$ and $f_{DOPC}^{Inner}(0)$ are the initial distribution ratio of PSM and DOPC, obtained from equation (1) and (2). $f_{PSM}^{Outer}(t_{max})$ and $f_{DOPC}^{Inner}(t_{max})$ are the limit values ($t \to \infty$), corresponding to the minimum experimental values.

The half-lives of the asymmetry ($t_{1/2}$) were obtained using Eq. 5.

$$t_{1/2} = \frac{ln2}{2k} \quad (5)$$

Further details are provided in Supporting Information.

■ RESULTS AND DISCUSSION

Optimization of MAS-ss-^{1}H NMR conditions. To optimize the experimental setup, MAS ^{1}H-ss-NMR was performed on symmetric LUVs (sLUVs) composed of POPC/Cho (7:3) (Fig.2). The spectrum measured at the MAS rate of 12 kHz showed a sharper $(CH_3)_3N^+$ peak at 3.21 ppm (Fig.2A) than that when spinning at 4 kHz. Hereafter, the MAS rate was set to 12 kHz unless otherwise specified. Upon addition of 1 mM Pr^{3+} (final concentration), a part of the $(CH_3)_3N^+$ peak of POPC shifted to a lower field (up to 3.25-3.30 ppm), while nearly half of the ^{1}H NMR signal originating from the inner leaflets did not change because Pr^{3+} did not approach the phospholipids in the inner leaflet (Fig. 2B).[30] Furthermore, the ratio of the two peak areas was 1:1, and their relaxation times were almost equal (Fig.S1). MAS ^{1}H-ss-NMR with 1 mM Pr^{3+} led to clear separation of the $(CH_3)_3N^+$ signal of POPC in the outer leaflet from that in the inner leaflet. Moreover, the peak-area ratios of these separated signals simply correspond to the outer/inner molar ratio of POPC because the effect of this paramagnetic reagent on the peak area was negligible under these conditions. Lanthanide ions are often reported to affect membrane properties. Pr^{3+} was added at each incubation time just prior to the NMR measurements, which were performed over a relatively short time period of 2–4 hours. Therefore, at the concentrations in this study, it is unlikely that the behavior of phospholipids would be significantly affected by Pr^{3+}. MAS during NMR measurements sometimes affect the properties of the membrane.

However, it would not significantly affect the NMR results for the same reason.

In this study, we added Cho to the aLUVs to mimic mammalian membranes, which also prevented gel-phase formation; the peak intensity of $(CH_3)_3N^+$ group was markedly reduced when the phospholipids are in the gel phase.[41] Formation of the fluid phase in aLUVs was confirmed by the temperature dependence of DPH anisotropy, with no abrupt change in anisotropy due to phase transition (Fig. S2).

MAS-ss-^{1}H NMR of aLUVs. NMR conditions optimized with the symmetric membranes were applied to determine the distribution ratio of phosphocholine lipids in each leaflet of the aLUVs. Prior to measurement, we determined the total lipid composition of aLUVs using solution ^{1}H NMR (See Supporting Information) of four separately prepared aLUV samples (PSM/DOPC/Cho = 38 ± 2: 37 ± 2: 26 ± 1, the mean ± standard error (SE) in mol %). However, 14~17 % of PSM turned out to be derived from donor MLVs that was contaminated during aLUV preparation; this fraction of PSM in the MLV was quantified by another experiment using nitrobenzoxadiazole(NBD)-Cho premixed in MLVs.[17,42] The remaining NBD fluorescence in the aLUV preparation revealed that most of unshifted PSM signal observed at 3.22 ppm in the presence of Pr^{3+} was due to MLV contamination (see Table S1 for details). On the other hand, PSM in the outermost leaflet of the residual MLV, which shows a peak shifted to 3.4 ppm, contributed only a small fraction of the peak area. Thus, we subtracted this fraction of PSM in the MLVs from the lipid composition ratio above. The modified lipid ratio of aLUVs thus obtained is as follows:

$$\text{PSM/DOPC/Cho} = 34 \pm 1 : 39 \pm 2 : 27 \pm 1 \qquad \text{(mol \%)}$$

Since a certain fraction of DOPC was oppositely transferred from LUV to donor multilamellar vesicles (MLVs), this DOPC fraction might affect the lipid composition. The percentage of transferred DOPC in the total aLUV lipids was estimated to be 2.6 mol% (see the legend for Table S1). Therefore, the effect of DOPC in the residual MLVs on the lipid composition of aLUVs can be considered within the margin of error. Furthermore, PSM in the outermost leaflet of the MLV contributed only a small fraction of the peak area which shows a peak shifted to 3.4 ppm (see Supporting Information for details). The aLUVs of γ-d_9-PSM^{out}/DOPC^{in}/Cho, where γ-d_9-PSM and DOPC were mostly present in the outer and inner leaflets of the vesicles, respectively (Table S1), were added with Pr^{3+} to selectively induce LIS on the outer leaflet (Fig.3). Superscripts 'in' and 'out' indicate the phospholipids present in the inner and outer leaflets of the vesicles, respectively. As shown in Fig.3A, the $(CH_3)_3N^+$ signal of DOPC was observed only at 3.21 ppm immediately after aLUVs preparation. After 10 h of incubation, however, an additional peak at 3.36 ppm appeared, and the peak intensity increased as the incubation time increased (Fig.3A, C, E, G). These data indicate that DOPC in the outer leaflet of the

acceptor LUVs was completely exchanged with PSM during the aLUV preparation, and during the incubation period, a portion of the DOPC was flopped from the inner leaflet to the outer leaflet.

The $(CH_3)_3N^+$ signal of PSM in aLUVs composed of PSM^{out}/γ-d_9-$DOPC^{in}$/Cho was observed in the presence of Pr^{3+} at 3.37 ppm and 3.22 ppm at the beginning of incubation (Fig.3B). As described above, this fraction of PSM was mostly due to the contamination of the remaining donor MLVs composed of PSM. The peak intensity at 3.22 ppm increased after incubation for 10 h and 40 h, indicating that PSM was partially flipped into the inner leaflet (Fig.3D, F), and it became almost the same as that at 3.37 ppm after incubation for 120 h, representing that PSM were equally present between the inner and outer leaflet (Fig.3H).

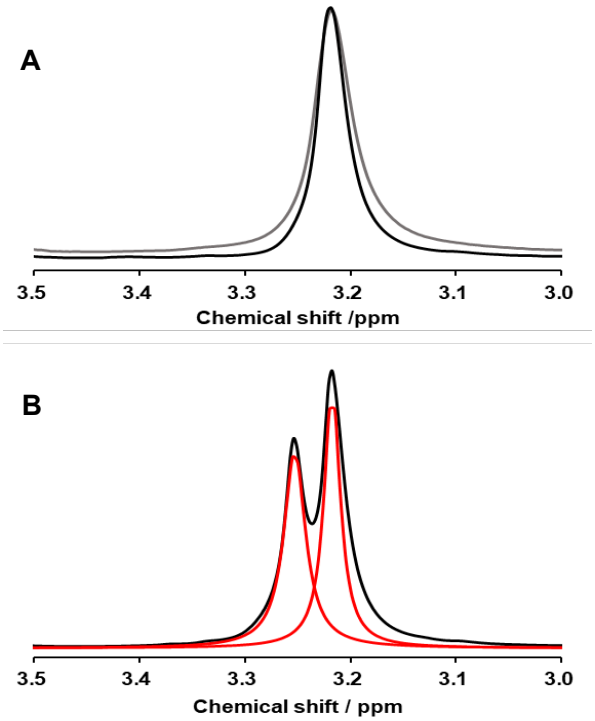

Figure 2. Trimethylammonium ($(CH_3)_3$-N^+) signals of POPC vesicles (0.9% NaCl in D_2O, 30 °C) in MAS-ss-^{1}H NMR spectra. **A,** MAS-ss-^{1}H NMR spectra of symmetric POPC/Cho (7:3) LUVs at the MAS rates of 4 kHz (gray trace) and 12 kHz (black trace), respectively. **B,** MAS ^{1}H-ss-NMR spectra of POPC/Cho (7:3) LUVs at 12 kHz MAS with 1 mM Pr^{3+} (black trace), and fitting curves (red traces). Spectra were recorded on an instrument with ^{1}H resonance frequency of 600 MHz. The lipid concentration was approximately 75 mM.

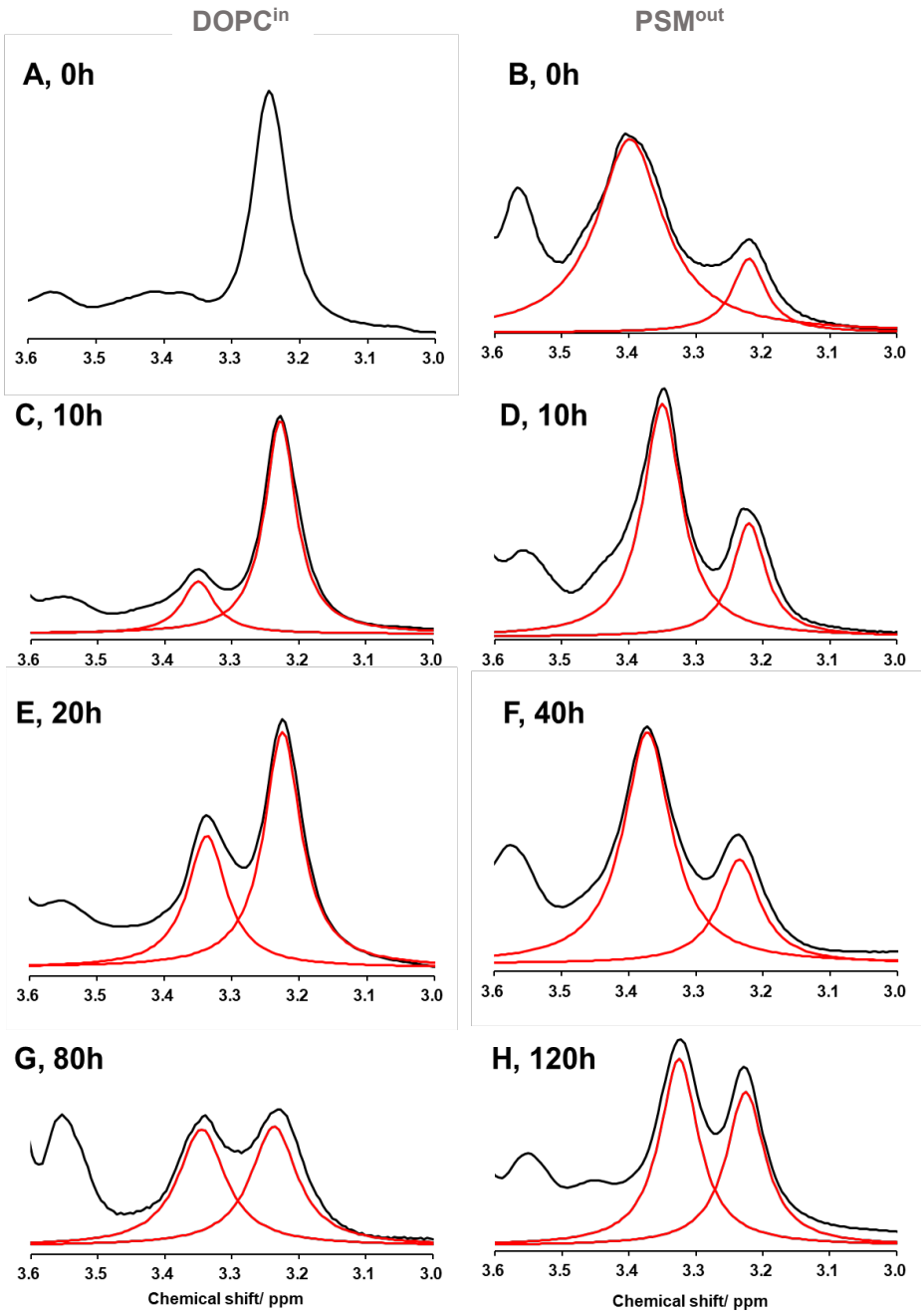

Figure 3. MAS-ss-^{1}H NMR spectra of the $(CH_3)_3N^+$ signals of aLUVs composed of PSM^{out}/DOPC^{in}/Cho in the presence of 1 mM Pr^{3+} in D_2O at 600 MHz (30 °C). **A**, **C, E, G**: The spectra of aLUVs composed of γ-d_9-PSM^{out}/DOPC^{in}/Cho were collected after incubation at 40 °C for 0 h (**A**), 10 h (**C**), 20 h (**E**) and 80 h (**G**). **B**, **D, F, H**: Spectra of aLUVs composed of PSM^{out}/γ-d_9-DOPC^{in}/Cho were recorded after incubation at 40 °C for 0 h (**B**), 10 h (**D**), 40 h (**F**) and 120 h (**H**). LIS by Pr^{3+}-induced down-field shifts of the $(CH_3)_3N^+$ signals (3.33-3.39 ppm) originated from the outer leaflet lipid. The slight differences in the down-fielded chemical shifts depended on the sample preparation including the molecular ratio of lipid and Pr^{3+}. The chemical shifts of the signal from inner leaf lipids, which were less affected by Pr^{3+}, were almost constant. The lipid concentrations of samples in the

NMR insert was estimated to be 10 mM to 50 mM. The additional peak at 3.55 ppm is from residual sucrose originating from aLUV preparation.

Lifetime of membrane asymmetry of aLUVs and sLUVs. The effect of membrane asymmetry on the flip-flop rate of lipids was estimated by comparing the aLUVs and sLUVs, the latter of which were actually asymmetric in terms of deuterated/not-deuterated lipids, even though they are symmetric in terms of lipid composition. The half-life ($t_{1/2}$) of the asymmetric lipid distribution, which approximately corresponds to the time required for 25 mol% lipid to translocate from one leaflet to the other, was measured based on time-dependent changes in the relative ratio of the $(CH_3)_3N^+$ peak areas from the inner and outer leaflets (Figure S2). To measure the flip-flop rate of phospholipids in symmetric lipid composition, we prepared the sLUVs consisting of PSM^{out}/γ-d_9-PSM^{in}/Cho and γ-d_9-$DOPC^{out}$/$DOPC^{in}$/Cho, which allowed the selective observation of the flip-flop of the outer and inner lipid signals, respectively. Time-dependent changes in the lipid contents in these sLUVs were measured by the same method as that for aLUVs.

As a result, a difference in the $t_{1/2}$ values of DOPC and PSM in the sLUVs (Fig.4B) indicated that DOPC more rapidly flops into the opposite leaflet compared to PSM. The similar difference was observed in aLUVs composed of PSM^{out}/$DOPC^{in}$/Cho (Fig.4A). These differences in flip-flop kinetics are assumed to correlate with the area per lipid. [14,43,44] Namely, the lateral lipid-lipid interactions occurring within each leaflet predominantly govern the lipid flip-flop rates, whereas the effect of asymmetry was considered relatively small. Additionally, a significant increase in the membrane order was observed in aLUVs after 120 h of incubation (Fig.5). Thus, gradual symmetrization of aLUVs probably resulted in the lateral segregation into the Ld and Lo phases in both leaflets,[45,46] which somehow affected the $t_{1/2}$ values[47,48] Actually, the apparent k values for DOPC and PSM obtained from the whole incubation period were 3.8×10^{-6} s^{-1} and 1.7×10^{-6} s^{-1}, respectively, which are somewhat smaller than those obtained from translocation rates in the first half of translocation (Table 1). As described below, we also obtained the same flip-flop rates for the first quarter, which were slightly larger than the values for the first half (Fig. S5C). However, since the error was large in these values, we used the kinetic parameters obtained from the first half of the incubation period in subsequent analyses to examine the effect of asymmetry on the flip-flop rate of aLUVs. The apparent k values of aLUVs were obtained for a longer period (1.7×10^{-6} s^{-1} for PSM and 3.8×10^{-6} s^{-1} for DOPC up to 120 h).

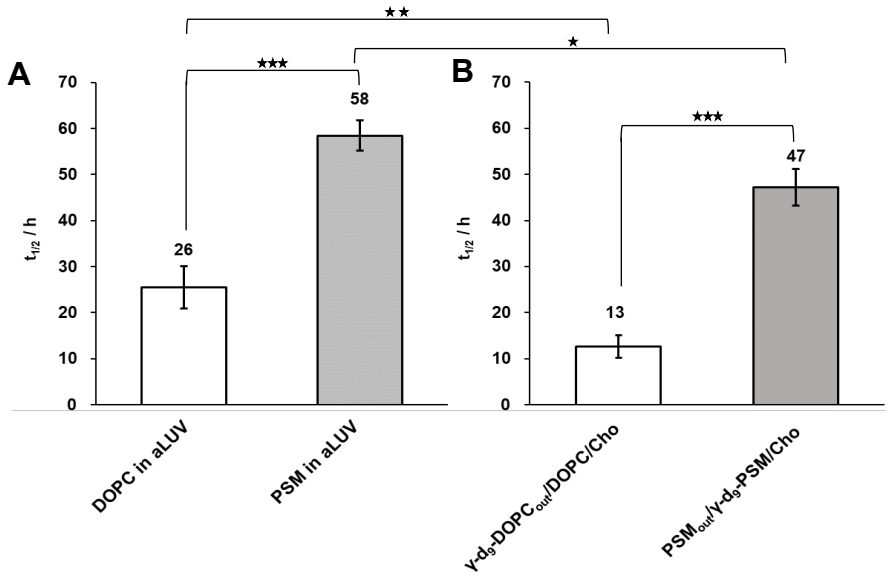

Figure 4. Half-lives of DOPC (*open bars*) and PSM (*gray bars*) in aLUVs (**A**) and sLUVs (**B**). aLUVs contained 27 mol% Cho. The Cho contents in PSM^{out}/γ-d_9-PSM^{in}/Cho and γ-d_9-DOPC^{out}/DOPC^{in}/Cho were 28 mol% and 21 mol%, respectively. Error bars represent the mean ± standard error (SE) of a set of n =8–22. Statistical significance was determined from student t-test. ★p<0.1, ★★p<0.05, ★★★p<0.01.

Table 1. Flip-flop rates of aLUVs and sLUVs. The flip-flop rates of aLUVs were deduced from the first half of the symmetrization process (until 50% of the PSM or DOPC was translocated). Errors in the mean values were obtained from the 95 % confidence interval calculated from SE × 1.96.

	Asymmetric LUVs (PSM/DOPC/Cho)		Symmetric LUVs (PSM/Cho or DOPC/Cho)	
Lipid	DOPC	PSM	DOPC	PSM
Flip-flop rate k ($\times 10^{-6}$ s^{-1})	6.4 ± 1.5	2.7 ± 0.8	7.7 ± 2.9	2.0 ± 0. 3

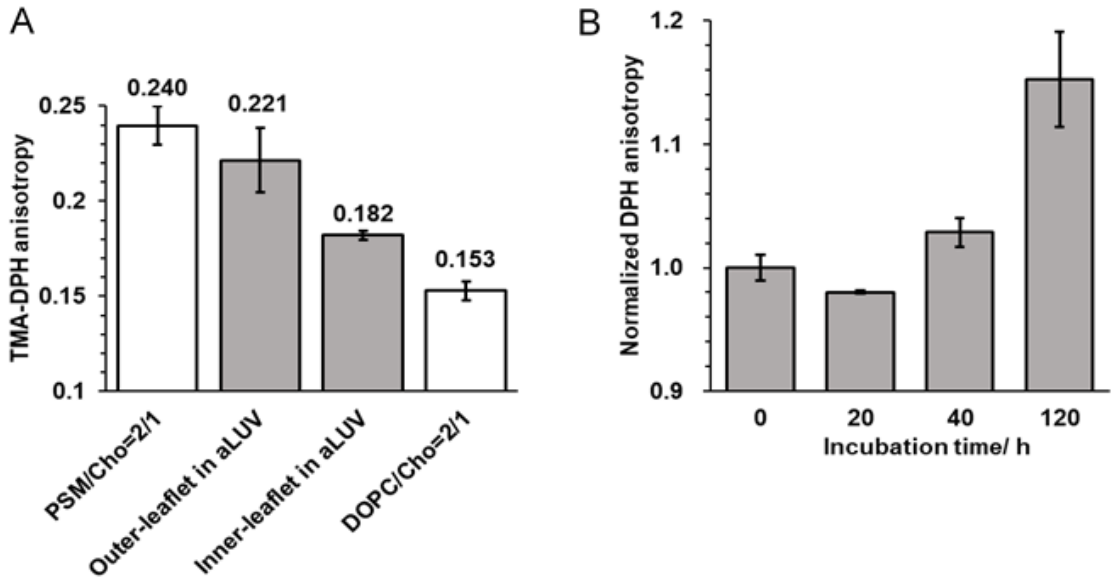

Figure 5. Fluorescence anisotropies of TMA-DPH in aLUVs and sLUVs (A), and time-course of change in DPH anisotropy in aLUVs (B). A, TMA-DPH anisotropy in sLUVs consisting of PSM/Cho 2:1 and DOPC/Cho 2:1 (*open bars*), and aLUVs (*filled bars*) at 40 °C. B, Time-dependent changes in DPH anisotropy at 40 °C in aLUVs, where DPH was present in both leaflets. The anisotropy values were normalized using the value at 0 h. Errors in the mean values were obtained from the 95% confidence interval calculated from SE × 1.96. Mean and SE values were obtained from triplicate preparations. The lipid concentration of the aLUV suspensions was approximately 100 μM based on fluorescence anisotropy measurements.

Flip-flop rates of aLUVs and sLUVs. The kinetic parameters of phospholipid flip-flops in bilayer membranes are important for gaining insights into homeostasis maintenance and the disruption of the asymmetry of biological membranes. To reduce the influence of domain formation during lipid flip-flop, the rate constants (k) for lipid translocation in aLUVs and sLUVs were measured from the first half of the decay curves (0% to 50% flip) (Table 1 and Fig. 6). The difference between PSM and DOPC in the flip-flop rate (Table 1, Fig. S3B) showed a similar trend to that in the $t_{1/2}$ values (Fig. 4). The flip-flop rates of PSM in aLUVs tended to be slightly higher than those in the binary sLUVs consisting of PSM/Cho. By contrast, the rates of DOPC showed a marginal difference between aLUVs and the sLUVs (Fig S3B, Table 1). This result suggests that the tight chain packing of PSM is more susceptible to the loose chain packing of DOPC on the other side as compared to the opposite case.

The reproducibility of the NMR experiments was rather low (Fig. S3A), mainly due to the intrinsic difficulty in preparing aLUVs with a constant lipid composition and in preventing MLV contamination; there were two cases of this contamination: coexisting donor MLVs and residual MLVs (and multivesicular vesicles) in acceptor LUVs. The latter case was not included in the correction of lipid composition because it is difficult to quantify. Therefore, the experiment was repeated at least

eight times to test the significance of the differences in flip-flop rates under each condition (Fig. 4).

It is noteworthy that the difference in Cho concentration among the LUV preparations was unlikely to influence the flip-flop kinetics in this experiment—Cho content of the vesicles consisting of PSM^{out}/γ-d_9-PSM^{in}/Cho was approximately 28 mol%, and that of the vesicles consisting of γ-d_9-DOPC^{out}/DOPC^{in}/Cho was 21 mol% by the solution NMR method (Table S2). This reduction in Cho content from the acceptor LUVs before lipid exchanges (33 mol%) may be largely caused by the MLV contamination, as discussed above. The difference in Cho content between PSM/DOPC/Cho and PSM^{out}/γ-d_9-PSM^{in}/Cho (or γ-d_9-DOPC^{out}/DOPC^{in}/Cho) may be due to the larger amount of the residual donor MLVs. However, since the Cho-induced ordering effect was not significant in this concentration range (Fig. S4), differences in Cho content among these LUVs were not considered to significantly affect the membrane properties that potentially affect the flip-flop rate. Therefore, we assumed that the differences in the flip-flop kinetics of the LUV preparations were largely due to factors other than Cho content.

As shown in Table 1, the flip-flop rates of DOPC were greater than those of PSM for both aLUVs and sLUVs. Previous studies have shown that the activation free energy of phospholipid flip-flop is strongly correlated with the molar compressive modulus and area per lipid.[14,43,44] Under the present conditions, DOPC bearing two unsaturated acyl chains has a larger area per lipid and smaller molar compressive modulus compared to PSM.[49,50,51] Therefore, the faster translocation rate of DOPC in Table 1 can be attributed to its smaller molar compressive modulus, which decreases the energy barrier for translocation. The similarity in the flip-flop rates of DOPC between aLUVs and sLUVs (Table 1) implies that lateral lipid-lipid interactions within the leaflet are a key factor in determining the lipid translocation rate. During flopping to the outer leaflet, DOPC invades the outer leaflet composed of PSM and spreads the mesh of the hydrogen bond network of the ordered PSM leaflet. However, the difference in the flip-flop rates of DOPC between the asymmetric and symmetric vesicles appears to be marginal in the present experiment. Further, when tightly packed PSMs in the outer leaflet are coupled with loosely packed DOPC in the inner leaflet, the PSM leaflet can be slightly relaxed while the DOPC leaflet may be slightly compressed to reduce mismatch.[52] This is also supported by the results of TMA-DPH anisotropy shown in Fig.5A. Therefore, the small differences in lipid translocation rates of PSM observed between aLUVs and sLUVs (Table 1) may be caused by certain changes in lateral lipid-lipid packing due to inter-leaflet interactions, which may influence the compressive modulus.

Cho effects on flip-flop rate. The present results showed that DOPC flip-flops faster than PSM, resulting in a higher number of phospholipids in the outer leaflet than in the inner leaflet of aLUVs. Since Cho flip-flops are much faster than phospholipids, their translocation to the opposite leaflet may relax overcrowding of outer leaflet phospholipids. To examine this possibility, we measured the time-

dependent change in the flip-flop rates over time (Fig. S3C). The results showed that the actual decreases in flip-flop rates were greater than the rate constants deduced from first-order kinetics, suggesting that Cho regulates the balance of lipid densities between the inner and outer leaflets under these experimental conditions. However, it is difficult to discuss the mechanism by which Cho regulates the flip-flop of phospholipids in detail, because the membrane leaflet distribution of Cho has not been precisely determined, even for artificial membranes. Therefore, further studies are warranted.

Cho is also known to exert the ordering effect either on the saturated and unsaturated acyl chains of phospholipids[53,54] although this effect varies depending on the unsaturation of acyl groups. Thus, the Cho content in bilayers should affect the flip-flop rate of phospholipids by changing the molar compressive modulus and area per lipid.[55] The distribution ratio of Cho in each leaflet of aLUVs is still under discussion. If content of Cho is significantly different between the inner and outer leaflets, it could influence the phospholipid flip-flop rate differently on PSM and DOPC. It is assumed that Cho possibly disrupts the SM hydrogen-bonding network and promotes fragmentation of SM gel-like domains in Lo domains,[56,57] which may promote the flip-flop of SM. By contrast, Cho residing in the liquid-disordered (Ld) phase increases the compressive modulus, thus potentially reducing the flip-flop rate of lipids in the Ld phase as seen for NBD-labeled lipid.[58] The present results indicate that aLUVs and sLUVs containing similar concentrations of total Cho have similar translocation rates of DOPC, which may imply that the distribution of Cho in the DOPC dominant inner leaflet of aLUVs may not be markedly different from that of sLUVs.

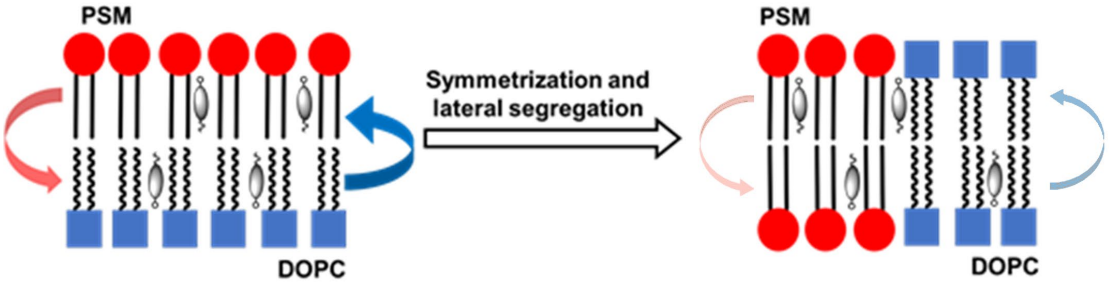

Figure 6. Schematic representation of the flip-flop kinetics of PSM and DOPC during symmetrization. The left (red) and right (blue) arrows represent the translocation of PSM and DOPC, respectively, with thick and thin arrows indicating higher and lower flip-flop rates, respectively. See Graphical Abstract for the symbol of lipid.

Flip-flop rates of PSM and DOPC compared with previous reports. The flip-flop rates of PSM and DOPC obtained in the present study are in the order of 10^{-5} to 10^{-6} s^{-1}, which are comparable with those of DPPC in LUVs observed by solution ^{1}H NMR,[30] but significantly slower than that obtained with phosphatidylcholine with an NBD-substituted acyl chain in vesicles (in the

order of 10^{-4} s^{-1} to 10^{-5} s^{-1}at 41 °C.[59] Substitution of an acyl chain with a hydrophobic and bulky fluorophore, which potentially disturbs the lateral chain packing, thus facilitating the flip-flop of the NBD lipid.

The flip-flop rates obtained in this study are slower than those of DPPC in supported bilayers (ca. 10^{-5} s^{-1}).[27,28] Previous Monte-Carlo simulations show that supported bilayers contain many submicron-sized defects, which may greatly accelerate the translocation of phospholipids between the leaflets.[30] Further, the compressive moduli of the planar bilayer are known to differ from those in the LUV bilayers.[60] Therefore, our study using LUVs may provide useful insights into the translocation rates for bilayer phospholipids in liposome environments.

Relevance to biological membranes. The asymmetric lipid distribution is highly conserved in the cell membranes of diverse organisms.[2,3] The lipid bilayers wrapping extracellular vesicles, such as exosomes, also exhibit asymmetry.[61,62] In addition to active lipid translocation by membrane proteins, the extremely slow rates via a thermodynamic process observed in this study may also be a key factor in maintaining asymmetric bilayers in cell membranes. For example, exposure of the PS to the cell surface, an important signal for phagocytosis and exosome markers,[10,11] likely takes very long time in spontaneous translocation and thus requires scramblases such as the chloride channel TMEM16.[61] The slow flip-flop of SM may also be important for the localization of diacylglycerol (DAG), which is involved in the immune function and the cell signal transduction.[63,64] It is reported that SM in the outer-leaflet decreases the trans-bilayer movement of DAG, which potentially suppresses DAG-induced activation of protein kinase C (PKC).[63,65] The cooperative regulation of membrane asymmetry via the passive process and enzyme-induced active transportation could help maintain basic functions of biological membranes. In particular, since it has been reported that changes in the local concentration of Cho may be involved in various biological phenomena[66,67] and amyloid-related diseases,[68] quantitative studies using model membranes on the distribution of Cho induced by asymmetric distribution of lipids are highly desirable. Although the effect of interleaflet interactions on PSM and DOPC translocation was not prominent under the present experimental conditions, further studies with other lipids and under other conditions are warranted.

■ CONCLUSION

Passive lipid translocation between bilayer leaflets is a fundamental process for scrambling asymmetric bilayers. Lipid translocation parameters such as the flip-flop rate have been used to evaluate the mechanisms that maintain cell membrane asymmetry; however, they are mostly obtained using lipid-type fluorescent probes, which sometimes behave differently from natural lipids. In the present study, the flip-flop rates of PSM and DOPC in aLUVs were estimated using MAS-ss-^{1}H NMR, with deuterated lipid probes bearing a $(CD_3)_3N^+$ group, since site-selective deuterium labeling has

little effect on the intrinsic membrane properties of phospholipids. The lateral lipid-lipid interactions dominantly governed the rate of phospholipid flip-flops (in the order of 10^{-6} s^{-1}), whereas the lipid composition of the opposite leaflet slightly affected the rate. Following previous studies using solution NMR,[19,30] the present study also revealed that MAS-ss-^{1}H NMR is a powerful tool for elucidating the asymmetric distribution and flip-flop events of phospholipids in asymmetric lipid bilayers. This method may lead to a better understanding of phospholipid behavior implicated in biological phenomena. The growing body of experimental data on aLUVs paves the way for a better understanding of the dynamic lipid properties of asymmetric bilayers. Some of the data can provide essential information for fine-tuning the molecular dynamics parameters to reproduce biomembrane dynamics.

■ ASSOCIATED CONTENT

Supporting Information

The Supporting Information is available free of charge at https://pubs.acs.org/doi/XXX. Detailed experimental data for determining lipid and cholesterol compositions and the additional experimental section including the synthesis of deuterated PSM and DOPC.

Conflicts of Interest

The authors declare no competing interests.

Acknowledgements

We are grateful to Prof. Erwin London, Stony Brook University for his guidance on experiments using asymmetric vesicles and to Drs. Inazumi and Todokoro, Osaka University for technical assistance in solid-state NMR spectroscopy. The UPLC-ESI-MS analysis was performed using research equipment shared in the MEXT Project for Promoting Public Utilization of Advanced Research Infrastructure (program for supporting construction of core facilities), Grant Number JPMXS0441200023, and we are also grateful for the technical assistance offered by Drs. Miyake, Osaka University. This work was supported in part by a Grant-in-Aid for Scientific Research A 21H04707 (M.M.) from the Japan Society for Promotion of Science (JSPS), CREST Grant Number JPMJCR18H2 (S.H.) from Japan Science and Technology Agency, and JST SPRING, Grant Number JPMJSP2138.

■ AUTHOR INFORMATION

Corresponding Authors

Shinya Hanashima− Graduate School of Engineering, Tottori University, 4-101 Koyama-cho Minami, Tottori 680-8550, Japan; orcid.org/0000-0003-3102-7890; Email: hanashima@tottori-u.ac.jp

Michio Murata − Department of Chemistry, Graduate School of Science, Osaka University, Toyonaka, Osaka 560- 0043, Japan; Forefront Research Center, Graduate School of Science, Osaka University, Toyonaka, Osaka 560-0043, Japan; orcid.org/0000-0002-1600-145X; Email: murata@chem.sci.osaka-u.ac.jp

Authors

Hirofumi Watanabe − Department of Chemistry, Graduate School of Science, Osaka University, Toyonaka, Osaka 560- 0043,Japan

Yo Yano − Department of Chemistry, Graduate, School of Science, Osaka University, Toyonaka, Osaka 560-0043, Japan.

Tomokazu Yasuda− Department of Chemistry, Graduate, School of Science, Osaka University, Toyonaka, Osaka 560-0043, Japan; Forefront Research Center, Graduate School of Science, Osaka University, Toyonaka, Osaka 560-0043, Japan

Author Contributions

H.W. mainly performed experiments with the guidance of S.H. and M.M. Y.Y. provided important techniques for preparing asymmetric bilayers. H.W. and H.S. designed the research. All authors interpreted data. H.W., S.H., and M. M. wrote the manuscript with input from all authors. All authors have approved the final version of the manuscript.

Note

Complete contact information is available at: https://pubs.acs.org/XXXX

References

(1) Bretscher, M. S. Asymmetrical Lipid Bilayer Structure for Biological Membranes. *Nature: New biology* **1972**, *236* (61), 11–12. https://doi.org/10.1038/newbio236011a0.

(2) Verkleij, A. J.; Zwaal, R. F.; Roelofsen, B.; Comfurius, P.; Kastelijn, D.; van Deenen, L. L. The Asymmetric Distribution of Phospholipids in the Human Red Cell Membrane. A Combined Study Using Phospholipases and Freeze-Etch Electron Microscopy. *Biochimica et biophysica acta* **1973**, *323* (2), 178–193. https://doi.org/10.1016/0005-2736(73)90143-0.

(3) Devaux, P. F. Static and Dynamic Lipid Asymmetry in Cell Membranes. *Biochemistry* **1991**, *30* (5), 1163–1173. https://doi.org/10.1021/bi00219a001.

(4) Murate, M.; Abe, M.; Kasahara, K.; Iwabuchi, K.; Umeda, M.; Kobayashi, T. Transbilayer Distribution of Lipids at Nano Scale. *Journal of cell science* **2015**, *128* (8), 1627–1638. https://doi.org/10.1242/jcs.163105.

(5) Seigneuret, M.; Devaux, P. F. ATP-Dependent Asymmetric Distribution of Spin-Labeled Phospholipids in the Erythrocyte Membrane: Relation to Shape Changes. *Proceedings of the National Academy of Sciences of the United States of America* **1984**, *81* (12), 3751–3755. https://doi.org/10.1073/pnas.81.12.3751.

(6) Kishimoto, T.; Mioka, T.; Itoh, E.; Williams, D. E.; Andersen, R. J.; Tanaka, K. Phospholipid Flippases and Sfk1 Are Essential for the Retention of Ergosterol in the Plasma Membrane. *Molecular biology of the cell* **2021**, *32* (15), 1374–1392. https://doi.org/10.1091/mbc.E20-11-

0699.

(7) Róg, T.; Vattulainen, I. Cholesterol, Sphingolipids, and Glycolipids: What Do We Know about Their Role in Raft-like Membranes? *Chemistry and physics of lipids* **2014**, *184*, 82–104. https://doi.org/10.1016/j.chemphyslip.2014.10.004.

(8) Simons, K.; van Meer, G. Lipid Sorting in Epithelial Cells. *Biochemistry* **1988**, *27* (17), 6197–6202. https://doi.org/10.1021/bi00417a001.

(9) Abe, M.; Makino, A.; Hullin-Matsuda, F.; Kamijo, K.; Ohno-Iwashita, Y.; Hanada, K.; Mizuno, H.; Miyawaki, A.; Kobayashi, T. A Role for Sphingomyelin-Rich Lipid Domains in the Accumulation of Phosphatidylinositol-4,5-Bisphosphate to the Cleavage Furrow during Cytokinesis. *Molecular and cellular biology* **2012**, *32* (8), 1396–1407. https://doi.org/10.1128/MCB.06113-11.

(10) Zwaal, R. F. A.; Comfurius, P.; Bevers, E. M. Surface Exposure of Phosphatidylserine in Pathological Cells. *Cellular and molecular life sciences : CMLS* **2005**, *62* (9), 971–988. https://doi.org/10.1007/s00018-005-4527-3.

(11) Skotland, T.; Sandvig, K.; Llorente, A. Lipids in Exosomes: Current Knowledge and the Way Forward. *Progress in lipid research* **2017**, *66*, 30–41. https://doi.org/10.1016/j.plipres.2017.03.001.

(12) Kawamoto, S.; Klein, M. L.; Shinoda, W. Coarse-Grained Molecular Dynamics Study of Membrane Fusion: Curvature Effects on Free Energy Barriers along the Stalk Mechanism. *The Journal of chemical physics* **2015**, *143* (24), 243112. https://doi.org/10.1063/1.4933087.

(13) Allhusen, J. S.; Kimball, D. R.; Conboy, J. C. Structural Origins of Cholesterol Accelerated Lipid Flip-Flop Studied by Sum-Frequency Vibrational Spectroscopy. *The journal of physical chemistry. B* **2016**, *120* (12), 3157–3168. https://doi.org/10.1021/acs.jpcb.6b01254.

(14) Sreekumari, A.; Lipowsky, R. Large Stress Asymmetries of Lipid Bilayers and Nanovesicles Generate Lipid Flip-Flops and Bilayer Instabilities. *Soft matter* **2022**, *18* (32), 6066–6078. https://doi.org/10.1039/d2sm00618a.

(15) Kato, U.; Inadome, H.; Yamamoto, M.; Emoto, K.; Kobayashi, T.; Umeda, M. Role for Phospholipid Flippase Complex of ATP8A1 and CDC50A Proteins in Cell Migration. *The Journal of biological chemistry* **2013**, *288* (7), 4922–4934. https://doi.org/10.1074/jbc.M112.402701.

(16) Kato, U.; Emoto, K.; Fredriksson, C.; Nakamura, H.; Ohta, A.; Kobayashi, T.; Murakami-Murofushi, K.; Kobayashi, T.; Umeda, M. A Novel Membrane Protein, Ros3p, Is Required for Phospholipid Translocation across the Plasma Membrane in Saccharomyces Cerevisiae. *The Journal of biological chemistry* **2002**, *277* (40), 37855–37862. https://doi.org/10.1074/jbc.M205564200.

(17) London, E. Membrane Structure-Function Insights from Asymmetric Lipid Vesicles. *Accounts of*

chemical research **2019**, *52* (8), 2382–2391. https://doi.org/10.1021/acs.accounts.9b00300.

(18) Pautot, S.; Frisken, B. J.; Weitz, D. A. Engineering Asymmetric Vesicles. *Proceedings of the National Academy of Sciences of the United States of America* **2003**, *100* (19), 10718–10721. https://doi.org/10.1073/pnas.1931005100.

(19) A. Heberle, F.; Marquardt, D.; Doktorova, M.; Geier, B.; F. Standaert, R.; Heftberger, P.; Kollmitzer, B.; D. Nickels, J.; A. Dick, R.; W. Feigenson, G.; Katsaras, J.; London, E.; Pabst, G. Subnanometer Structure of an Asymmetric Model Membrane: Interleaflet Coupling Influences Domain Properties. *Langmuir* **2016**, *32* (20), 5195–5200. https://doi.org/10.1021/acs.langmuir.5b04562.

(20) Sun, H.-Y.; Deng, G.; Jiang, Y.-W.; Zhou, Y.; Xu, J.; Wu, F.-G.; Yu, Z.-W. Controllable Engineering of Asymmetric Phosphatidylserine-Containing Lipid Vesicles Using Calcium Cations. *Chem. Commun.* **2017**, *53* (95), 12762–12765. https://doi.org/10.1039/C7CC05114J.

(21) Guo, H.-Y.; Sun, H.-Y.; Deng, G.; Xu, J.; Wu, F.-G.; Yu, Z.-W. Fabrication of Asymmetric Phosphatidylserine-Containing Lipid Vesicles: A Study on the Effects of Size, Temperature, and Lipid Composition. *Langmuir* **2020**, *36* (42), 12684–12691. https://doi.org/10.1021/acs.langmuir.0c02273.

(22) Takaoka, R.; Kurosaki, H.; Nakao, H.; Ikeda, K.; Nakano, M. Formation of Asymmetric Vesicles via Phospholipase D-Mediated Transphosphatidylation. *Biochimica et biophysica acta. Biomembranes* **2018**, *1860* (2), 245–249. https://doi.org/10.1016/j.bbamem.2017.10.011.

(23) Drechsler, C.; Markones, M.; Choi, J.-Y.; Frieling, N.; Fiedler, S.; Voelker, D. R.; Schubert, R.; Heerklotz, H. Preparation of Asymmetric Liposomes Using a Phosphatidylserine Decarboxylase. *Biophysical journal* **2018**, *115* (8), 1509–1517. https://doi.org/10.1016/j.bpj.2018.08.036.

(24) Doktorova, M.; Heberle, F. A.; Eicher, B.; Standaert, R. F.; Katsaras, J.; London, E.; Pabst, G.; Marquardt, D. Preparation of Asymmetric Phospholipid Vesicles for Use as Cell Membrane Models. *Nature protocols* **2018**, *13* (9), 2086–2101. https://doi.org/10.1038/s41596-018-0033-6.

(25) Wang, Q.; London, E. Lipid Structure and Composition Control Consequences of Interleaflet Coupling in Asymmetric Vesicles. *Biophysical journal* **2018**, *115* (4), 664–678. https://doi.org/10.1016/j.bpj.2018.07.011.

(26) McIntyre, J. C.; Sleight, R. G. Fluorescence Assay for Phospholipid Membrane Asymmetry. *Biochemistry* **1991**, *30* (51), 11819–11827. https://doi.org/10.1021/bi00115a012.

(27) Liu, J.; Brown, K. L.; Conboy, J. C. The Effect of Cholesterol on the Intrinsic Rate of Lipid Flip-Flop as Measured by Sum-Frequency Vibrational Spectroscopy. *Faraday discussions* **2013**, *161*, 45–50. https://doi.org/10.1039/c2fd20083j.

(28) Liu, J.; Conboy, J. C. 1,2-Diacyl-Phosphatidylcholine Flip-Flop Measured Directly by Sum-Frequency Vibrational Spectroscopy. *Biophysical journal* **2005**, *89* (4), 2522–2532. https://doi.org/10.1529/biophysj.105.065672.

(29) Tieleman, D. P.; Marrink, S.-J. Lipids out of Equilibrium: Energetics of Desorption and Pore Mediated Flip-Flop. *Journal of the American Chemical Society* **2006**, *128* (38), 12462–12467. https://doi.org/10.1021/ja0624321.

(30) Marquardt, D.; Heberle, F. A.; Miti, T.; Eicher, B.; London, E.; Katsaras, J.; Pabst, G. (1)H NMR Shows Slow Phospholipid Flip-Flop in Gel and Fluid Bilayers. *Langmuir : the ACS journal of surfaces and colloids* **2017**, *33* (15), 3731–3741. https://doi.org/10.1021/acs.langmuir.6b04485.

(31) Perly, B.; Smith, I. C.; Hughes, L.; Burton, G. W.; Ingold, K. U. Estimation of the Location of Natural Alpha-Tocopherol in Lipid Bilayers by 13C-NMR Spectroscopy. *Biochimica et biophysica acta* **1985**, *819* (1), 131–135. https://doi.org/10.1016/0005-2736(85)90203-2.

(32) Yamamoto, T.; Umegawa, Y.; Tsuchikawa, H.; Hanashima, S.; Matsumori, N.; Funahashi, K.; Seo, S.; Shinoda, W.; Murata, M. The Amphotericin B-Ergosterol Complex Spans a Lipid Bilayer as a Single-Length Assembly. *Biochemistry* **2019**, *58* (51), 5188–5196. https://doi.org/10.1021/acs.biochem.9b00835.

(33) Hunt, G. R. Kinetics of Ionophore-Mediated Transport of Pr3+ Ions through Phospholipid Membranes Using 1h NMR Spectroscopy. *FEBS letters* **1975**, *58* (1), 194–196. https://doi.org/10.1016/0014-5793(75)80257-2.

(34) Weybright, P.; Millis, K.; Campbell, N.; Cory, D. G.; Singer, S. Gradient, High-Resolution, Magic Angle Spinning 1H Nuclear Magnetic Resonance Spectroscopy of Intact Cells. *Magnetic resonance in medicine* **1998**, *39* (3), 337–345. https://doi.org/10.1002/mrm.1910390302.

(35) Huxley, A. F.; Simmons, R. M. Proposed Mechanism of Force Generation in Striated Muscle. *Nature* **1971**, *233* (5321), 533–538. https://doi.org/10.1038/233533a0.

(36) Su, Y.; Mani, R.; Hong, M. Asymmetric Insertion of Membrane Proteins in Lipid Bilayers by Solid-State NMR Paramagnetic Relaxation Enhancement: A Cell-Penetrating Peptide Example. *Journal of the American Chemical Society* **2008**, *130* (27), 8856–8864. https://doi.org/10.1021/ja802383t.

(37) Umegawa, Y.; Yamamoto, T.; Dixit, M.; Funahashi, K.; Seo, S.; Nakagawa, Y.; Suzuki, T.; Matsuoka, S.; Tsuchikawa, H.; Hanashima, S.; Oishi, T.; Matsumori, N.; Shinoda, W.; Murata, M. Amphotericin B Assembles into Seven-Molecule Ion Channels: An NMR and Molecular Dynamics Study. *Science Advances* **2022**, *8* (24), 1–11. https://doi.org/10.1126/sciadv.abo2658.

(38) Matsumori, N.; Yasuda, T.; Okazaki, H.; Suzuki, T.; Yamaguchi, T.; Tsuchikawa, H.; Doi, M.; Oishi, T.; Murata, M. Comprehensive Molecular Motion Capture for Sphingomyelin by Site-Specific Deuterium Labeling. *Biochemistry* **2012**, *51* (42), 8363–8370. https://doi.org/10.1021/bi3009399.

(39) Yasuda, T.; Al Sazzad, M. A.; Jäntti, N. Z.; Pentikäinen, O. T.; Slotte, J. P. The Influence of Hydrogen Bonding on Sphingomyelin/Colipid Interactions in Bilayer Membranes. *Biophysical Journal* **2016**. https://doi.org/10.1016/j.bpj.2015.11.3515.

(40) Cheng, V.; Conboy, J. C. Inhibitory Effect of Lanthanides on Native Lipid Flip-Flop. *The Journal of Physical Chemistry B* **2022**, *126* (39), 7651–7663. https://doi.org/10.1021/acs.jpcb.2c04039.

(41) Pentak, D. Alternative Methods of Determining Phase Transition Temperatures of Phospholipids That Constitute Liposomes on the Example of DPPC and DMPC. *Thermochimica Acta* **2014**, *584*, 36–44. https://doi.org/https://doi.org/10.1016/j.tca.2014.03.020.

(42) Ohtani, Y.; Irie, T.; Uekama, K.; Fukunaga, K.; Pitha, J. Differential Effects of Alpha-, Beta- and Gamma-Cyclodextrins on Human Erythrocytes. *European journal of biochemistry* **1989**, *186* (1–2), 17–22. https://doi.org/10.1111/j.1432-1033.1989.tb15171.x.

(43) Anglin, T. C.; Conboy, J. C. Lateral Pressure Dependence of the Phospholipid Transmembrane Diffusion Rate in Planar-Supported Lipid Bilayers. *Biophysical journal* **2008**, *95* (1), 186–193. https://doi.org/10.1529/biophysj.107.118976.

(44) Anglin, T. C.; Conboy, J. C. Kinetics and Thermodynamics of Flip-Flop in Binary Phospholipid Membranes Measured by Sum-Frequency Vibrational Spectroscopy. *Biochemistry* **2009**, *48* (43), 10220–10234. https://doi.org/10.1021/bi901096j.

(45) Lin, Q.; London, E. Ordered Raft Domains Induced by Outer Leaflet Sphingomyelin in Cholesterol-Rich Asymmetric Vesicles. *Biophysical Journal* **2015**, *108* (9), 2212–2222. https://doi.org/10.1016/j.bpj.2015.03.056.

(46) St Clair, J. W.; Kakuda, S.; London, E. Induction of Ordered Lipid Raft Domain Formation by Loss of Lipid Asymmetry. *Biophysical journal* **2020**, *119* (3), 483–492. https://doi.org/10.1016/j.bpj.2020.06.030.

(47) Kučerka, N.; Nieh, M.-P.; Katsaras, J. Fluid Phase Lipid Areas and Bilayer Thicknesses of Commonly Used Phosphatidylcholines as a Function of Temperature. *Biochimica et biophysica acta* **2011**, *1808* (11), 2761–2771. https://doi.org/10.1016/j.bbamem.2011.07.022.

(48) Armstrong, C. L.; Marquardt, D.; Dies, H.; Kučerka, N.; Yamani, Z.; Harroun, T. A.; Katsaras, J.; Shi, A.-C.; Rheinstädter, M. C. The Observation of Highly Ordered Domains in Membranes with Cholesterol. *PloS one* **2013**, *8* (6), e66162. https://doi.org/10.1371/journal.pone.0066162.

(49) Venable, R. M.; Brown, F. L. H.; Pastor, R. W. Mechanical Properties of Lipid Bilayers from Molecular Dynamics Simulation. *Chemistry and physics of lipids* **2015**, *192*, 60–74. https://doi.org/10.1016/j.chemphyslip.2015.07.014.

(50) Kucerka, N.; Tristram-Nagle, S.; Nagle, J. F. Structure of Fully Hydrated Fluid Phase Lipid Bilayers with Monounsaturated Chains. *The Journal of membrane biology* **2005**, *208* (3), 193–202. https://doi.org/10.1007/s00232-005-7006-8.

(51) Hanashima, S.; Ibata, Y.; Watanabe, H.; Yasuda, T.; Tsuchikawa, H.; Murata, M. Side-Chain Deuterated Cholesterol as a Molecular Probe to Determine Membrane Order and Cholesterol Partitioning. *Organic and Biomolecular Chemistry* **2019**, *17* (37). https://doi.org/10.1039/c9ob01342c.

(52) Doktorova, M.; Symons, J. L.; Levental, I. Structural and Functional Consequences of Reversible Lipid Asymmetry in Living Membranes. *Nature chemical biology* **2020**, *16* (12), 1321–1330. https://doi.org/10.1038/s41589-020-00688-0.

(53) Yasuda, T.; Kinoshita, M.; Murata, M.; Matsumori, N. Detailed Comparison of Deuterium Quadrupole Profiles between Sphingomyelin and Phosphatidylcholine Bilayers. *Biophysical Journal* **2014**, *106* (3), 631–638. https://doi.org/10.1016/j.bpj.2013.12.034.

(54) Yasuda, T.; Tsuchikawa, H.; Murata, M.; Matsumori, N. Deuterium NMR of Raft Model Membranes Reveals Domain-Specific Order Profiles and Compositional Distribution. *Biophysical Journal* **2015**, *108* (10), 2502–2506. https://doi.org/10.1016/j.bpj.2015.04.008.

(55) Allhusen, J. S.; Conboy, J. C. The Ins and Outs of Lipid Flip-Flop. *Accounts of chemical research* **2017**, *50* (1), 58–65. https://doi.org/10.1021/acs.accounts.6b00435.

(56) Yano, Y.; Hanashima, S.; Yasuda, T.; Tsuchikawa, H.; Matsumori, N.; Kinoshita, M.; Al Sazzad, M. A.; Slotte, J. P.; Murata, M. Sphingomyelin Stereoisomers Reveal That Homophilic Interactions Cause Nanodomain Formation. *Biophysical Journal* **2018**, *115* (8), 1530–1540. https://doi.org/10.1016/j.bpj.2018.08.042.

(57) Murata, M.; Matsumori, N.; Masanao Kinoshita, ·; London, E. Molecular Substructure of the Liquid-Ordered Phase Formed by Sphingomyelin and Cholesterol: Sphingomyelin Clusters Forming Nano-Subdomains Are a Characteristic Feature. *Biophysical Reviews 1*, 3. https://doi.org/10.1007/s12551-022-00967-1.

(58) Kol, M. A.; van Laak, A. N. C.; Rijkers, D. T. S.; Killian, J. A.; de Kroon, A. I. P. M.; de Kruijff, B. Phospholipid Flop Induced by Transmembrane Peptides in Model Membranes Is Modulated by Lipid Composition. *Biochemistry* **2003**, *42* (1), 231–237. https://doi.org/10.1021/bi0268403.

(59) John, K.; Schreiber, S.; Kubelt, J.; Herrmann, A.; Müller, P. Transbilayer Movement of Phospholipids at the Main Phase Transition of Lipid Membranes: Implications for Rapid Flip-Flop in Biological Membranes. *Biophysical Journal* **2002**, *83* (6), 3315–3323. https://doi.org/https://doi.org/10.1016/S0006-3495(02)75332-0.

(60) Makino, K.; Shibata, A. Chapter 2: Surface Properties of Liposomes Depending on Their Composition; Liu, A. L., Ed.; Advances in Planar Lipid Bilayers and Liposomes; Academic Press, 2006; Vol. 4, pp 49–77. https://doi.org/https://doi.org/10.1016/S1554-4516(06)04002-6.

(61) Falzone, M. E.; Feng, Z.; Alvarenga, O. E.; Pan, Y.; Lee, B.; Cheng, X.; Fortea, E.; Scheuring, S.; Accardi, A. TMEM16 Scramblases Thin the Membrane to Enable Lipid Scrambling. *Nature communications* **2022**, *13* (1), 2604. https://doi.org/10.1038/s41467-022-30300-z.

(62) Yasuda, T.; Watanabe, H.; Hirosawa, K. M.; Suzuki, K. G. N.; Suga, K.; Hanashima, S. Fluorescence Spectroscopic Analysis of Lateral and Transbilayer Fluidity of Exosome Membranes. *Langmuir : the ACS journal of surfaces and colloids* **2022**, *38* (48), 14695–14703. https://doi.org/10.1021/acs.langmuir.2c02258.

(63) Ueda, Y.; Makino, A.; Murase-Tamada, K.; Sakai, S.; Inaba, T.; Hullin-Matsuda, F.; Kobayashi, T. Sphingomyelin Regulates the Transbilayer Movement of Diacylglycerol in the Plasma Membrane of Madin-Darby Canine Kidney Cells. *FASEB journal : official publication of the Federation of American Societies for Experimental Biology* **2013**, *27* (8), 3284–3297. https://doi.org/10.1096/fj.12-226548.

(64) Gharbi, S. I.; Rincón, E.; Avila-Flores, A.; Torres-Ayuso, P.; Almena, M.; Cobos, M. A.; Albar, J. P.; Mérida, I. Diacylglycerol Kinase ζ Controls Diacylglycerol Metabolism at the Immunological Synapse. *Molecular biology of the cell* **2011**, *22* (22), 4406–4414. https://doi.org/10.1091/mbc.E11-03-0247.

(65) Schmidt, A. M.; Zou, T.; Joshi, R. P.; Leichner, T. M.; Pimentel, M. A.; Sommers, C. L.; Kambayashi, T. Diacylglycerol Kinase ζ Limits the Generation of Natural Regulatory T Cells. *Science signaling* **2013**, *6* (303), ra101. https://doi.org/10.1126/scisignal.2004411.

(66) Wood, W. G.; Igbavboa, U.; Müller, W. E.; Eckert, G. P. Cholesterol Asymmetry in Synaptic Plasma Membranes. *Journal of neurochemistry* **2011**, *116* (5), 684–689. https://doi.org/10.1111/j.1471-4159.2010.07017.x.

(67) Ogasawara, F.; Ueda, K. ABCA1 and Cholesterol Transfer Protein Aster-A Promote an Asymmetric Cholesterol Distribution in the Plasma Membrane. *The Journal of biological chemistry* **2022**, *298* (12), 102702. https://doi.org/10.1016/j.jbc.2022.102702.

(68) Sciacca, M. F. M.; Lolicato, F.; Di Mauro, G.; Milardi, D.; D'Urso, L.; Satriano, C.; Ramamoorthy, A.; La Rosa, C. The Role of Cholesterol in Driving IAPP-Membrane Interactions. *Biophysical journal* **2016**, *111* (1), 140–151. https://doi.org/10.1016/j.bpj.2016.05.050.

Graphical Abstract TOC graphic